

# Rotating bed reactor for CLC; bed characteristics dependencies on internal gas mixing

Silje Fosse HÅKONSEN, Carlos A. GRANDE & Richard BLOM \*

*SINTEF Materials & Chemistry, P. O. Box 124 Blindern, N-0314 Oslo, Norway*

\*Corresponding Author; [Richard.blom@sintef.no](mailto:Richard.blom@sintef.no), tel. +47 90622647, fax. +47 22067350

## Abstract:

A newly designed continuous lab-scale rotating bed reactor for chemical looping combustion using CuO/Al<sub>2</sub>O<sub>3</sub> oxygen carrier spheres and methane as fuel gives around 90% CH<sub>4</sub> conversion and >90% CO<sub>2</sub> capture efficiency based on converted methane at 800°C. However, from a series of experiments using a broad range of operating conditions potential CO<sub>2</sub> purities only in the range 20-65% were yielded, mostly due to nitrogen slippage from the air side of the reactor into the effluent CO<sub>2</sub> stream. A mathematical model was developed intending to understand the air-mixing phenomena. The model clearly reflects the gas slippage tendencies observed when varying the process conditions such as rotation frequency, gas flow and the flow of inert gas in the two sectors dividing the air and fuel side of the reactor. Based on the results, it is believed that significant improvements can be made to reduce gas mixing in future modified and scaled-up reactor versions.

**Keywords:** CO<sub>2</sub> capture; Chemical looping combustion; continuous operation; rotating bed reactor; reactor modeling; oxygen carrier

## 1 Introduction

A chemical looping combustion (CLC) process was already suggested in the 1950's as a way to produce pure carbon dioxide [1]. It was further developed as a combustion technique in the 1980's [2], and later in the 1990's presented as a possible way to separate CO<sub>2</sub> during fossil fuel combustion [3]. The interest in CLC has boosted during the last decade due to its relatively high net energy efficiency [4,5] and potential low cost of CO<sub>2</sub> capture [6] and an early review by de Lasa et al [7] has recently been followed up by a number of reviews covering the field [8,9,10].

CLC is a cyclic process where a metal oxide first is used to combust a fuel, and then the reduced metal oxide is re-oxidation in air before a new cycle can be carried out. Either the metal oxide is moved (or circulated) between static gas streams, or the gas composition is changed while keeping the metal oxide static. Option i) is in most cases implemented by a circulating fluidized bed (CFB) reactor setup where the metal oxide powder circulates between a fuel reactor in which the combustion takes place and an air reactor where re-oxidation takes place [11,12]. CFB reactors have recently gained far the most attention within the CLC community since this reactor type already is commercial for combustion processes (boilers) and within refinery processes such as fluidized catalytic cracking (FCC). Option ii) most often involves one or more fixed bed reactors where complex valving sequences assure cyclic gas feeding to the reactors and optimal gas separation. Early CLC experiments were carried out in single fixed bed reactors [3,13].

We have recently developed an alternative reactor concept for CLC which belongs to the option i) group above in which the metal oxide is kept in a doughnut shaped fixed bed that rotates between different radially flowing gas streams. The reactor is shown in Figure 1. The gases are fed through porous metal walls on the (fixed) central axis (see Figure 1 b) to assure even gas distribution in each feeding sector. A fuel sector of 60° and an air sector of 240° have been chosen, with inert sectors of 30° in-between. A 1:4 ratio between the fuel and air sectors is chosen as a compromise considering the stoichiometry of the reactions taking place ( $\text{CH}_4/\text{O}_2 = \frac{1}{2}$ ), the 21% concentration of O<sub>2</sub> in air, and the fact that we intended to use diluted CH<sub>4</sub> as feed in the fuel sector (typically from 10 to 50 vol% in argon). We have in an earlier communication described the basics of our rotating bed reactor system showing that separation of the gases is possible, although some internal gas mixing do occur [14]. Later we presented results from the first series of continuous CLC experiments carried out at elevated temperatures [15]. The results from these experiments will form the experimental

basis for the present paper where we will look closer into the main sources of internal gas mixing in such a reactor: First a thorough examination of the earlier experimental data with respect to internal gas mixing will be done. Secondly, results from mathematical modeling will be used to describe the main reasons for the observed internal gas mixing and some suggestions on how to minimize the gas mixing will be suggested.

<Figure 1>

## 2 Internal gas mixing within prototype reactor

### 2.1 Trends from continuous CLC experiments

Supported copper oxide ( $\text{CuO}/\text{Al}_2\text{O}_3$ ) spheres having approximately 1.5 mm diameter has so far been used as oxygen carrier for the rotating bed reactor [14]. CuO has been chosen mainly because both the reduction reaction ( $4\text{CuO} + \text{CH}_4 \rightarrow \text{CO}_2 + 2\text{H}_2\text{O} + 4\text{Cu}$ ;  $\Delta H^\circ = -206$  kJ/mol) and the re-oxidation reaction ( $4\text{Cu} + 2\text{O}_2 \rightarrow 4\text{CuO}$ ;  $\Delta H^\circ = -596$  kJ/mol) are exothermic thus minimizing large temperature gradients within the rotating bed [14]. Process parameters such as reactor temperature (700-800°C), bed rotating frequency (0-4 rotations/min) and gas flows (total flows between 800 and 2000 ml/min) were varied to find optimal performance of the prototype reactor. In the initial experiments dry air was used at the air side,  $\text{CH}_4$  dilutes with argon was used at the fuel side, and argon was used in both inert sectors. The total flow in each sector was proportional to the sector size, except in some cases where the argon flow in the two inert sectors was higher to see the effect of this on the separation efficiency. Around 90%  $\text{CH}_4$  conversion and >90%  $\text{CO}_2$  capture efficiency based on converted methane can be obtained with the prototype. Stable operation has been accomplished over several hours, and also – stable operation can be regained after intentionally running into unstable conditions. It is of importance that relatively high radial gas velocities are used to avoid fully reduced oxygen carrier in part of the bed. If we define the  $\text{CO}_2$  purity as the percentage of  $\text{CO}_2$  measured in the exit gas on the fuel side neglecting the argon present (since argon used in the experiments is a substitute for steam that can be condensed out) we find potential  $\text{CO}_2$  purities in the experiments ranging 20 to 65%.

In Figure 2 we show the dependencies of the potential  $\text{CO}_2$  purity on various process parameters. Some clear trends are observed. In the following section we will describe a mathematical model of the rotating bed reactor and some simulations that have been carried out to get further insight into the main reasons for internal gas mixing. The main aim of the present paper is to see how well the simulations reflect the experimental results. Secondly,

we will use the simulation results to give direction for both future reactor design improvements (geometry, tube sizing, etc.) and also more optimal oxygen carrier particle characteristics (porosity, sphere size, etc.)

<Figure 2>

### 3 Reactor modeling

#### 3.1 Mathematical model

The mathematical model of the reactor was developed to assess the effects of mass transfer coupled with momentum transfer and for this reason in this initial stage, the model assumes that the process is isothermal and that mass transfer resistances for gas diffusion are not important but reaction rate limited. The partial differential equations (PDE) were solved in COMSOL Multiphysics (COMSOL AB, Sweden). The domain definition of the reactor is shown in Figure 3 below.

<Figure 3>

The reactor has a main air inlet to oxidize the oxygen carrier and a fuel inlet where the Cu-carrier is reduced. The rotating reactor (bed filled with porous particles) is defined in sections 1a to 1d while the different sections of the reactor are gas chambers. The main complexity in modeling the reactor is that the rotation should be described in radial coordinates, which is differently from other reactor configurations where 1D models in the axial direction can provide a good description of the system [16,17].

The momentum equation in the reactor is defined by (Brinkman equation):

$$\left(\frac{\rho}{\varepsilon_c}\right) \frac{\partial \mathbf{u}}{\partial t} + \left(\frac{\eta}{\kappa_r}\right) \mathbf{u} = \nabla \left[ -p\mathbf{I} + \frac{1}{\varepsilon_c} \left\{ (\eta \nabla \mathbf{u} + (\nabla \mathbf{u})^T) - \frac{2\eta}{3} (\nabla \cdot \mathbf{u}) \mathbf{I} \right\} \right] + \mathbf{F} \quad (1)$$

where  $\varepsilon_c$  is the bed porosity and  $\kappa_r$  is the permeability of the rotating reactor. In the gas-phase sectors, the Navier – Stokes equation was used:

$$\rho \frac{\partial \mathbf{u}}{\partial t} + \rho (\mathbf{u} \cdot \nabla) \mathbf{u} = \nabla [-p\mathbf{I} + \eta (\nabla \mathbf{u} + (\nabla \mathbf{u})^T)] \quad (2)$$

where  $\rho$  is the gas density,  $p$  is the pressure and  $\eta$  is the gas viscosity. Rotational forces per unit volume in the bed (sections 1a-1d) are described by:

$$F_x = (1 - \varepsilon_c) \rho_p \omega^2 \sqrt{x^2 + y^2} \sin(\text{atan2}(y, x)) \quad (3)$$

$$F_y = (1 - \varepsilon_c)\rho_p\omega^2\sqrt{x^2 + y^2}\cos(\text{atan2}(y,x)) \quad (4)$$

where  $\rho_p$  is the density of the oxygen-carrier particles and  $\omega$  is the angular velocity.

The mass balance in the reactor is given by:

$$\delta_{TS}\frac{\partial C_i}{\partial t} + \nabla \cdot (-D\nabla C_i) = R - \mathbf{u}\nabla C_i \quad (5)$$

where  $C_i$  is the gas concentration of component  $i$  (valid for all species),  $u$  is the linear gas velocity and  $D$  is the dispersion coefficient. In the gas sections,  $D = D_m$  (molecular diffusion coefficient) while for the oxygen carrier bed,  $D = D_r$  (bed dispersion coefficient). The bed dispersion coefficient has radial (flow direction) and angular components. The radial component was calculated by:

$$D_r = 2(0.45 + 0.55\varepsilon_r)D_m + R_p u_{feed} \quad (6)$$

where  $u_{feed}$  is the inlet gas velocity in the rotating reactor. Although this equation was developed for fixed beds, with the particle diameter ( $1.5 \times 10^{-4}$  m) and the velocity values used in this study ( $5.5 \times 10^{-3}$  m/s), the bed dispersion is mainly controlled by the molecular diffusion coefficient ( $\sim 1 \times 10^{-4}$  m<sup>2</sup>/s).

The time-coefficient  $\delta_{TS}$  also changes with position being:  $\delta_{TS} = 1$  in the gas sections and  $\delta_{TS} = \varepsilon_c$  inside the reactor. The rate term,  $R$ , in the gas sections is  $R = 0$  while inside the rotating bed is described as:

$$R = (1 - \varepsilon_c)a_p K_G (C_i - \overline{C}_{p_i}) \quad (7)$$

where  $K_G$  is the global mass transfer resistance and  $a_p$  is the area to volume ratio of the particles of catalyst ( $a_p = \frac{3}{R_p}$  for spherical particles). The averaged concentration of component  $i$  inside the particles ( $\overline{C}_{p_i}$ ) is given by:

$$\varepsilon_p \frac{\partial \overline{C}_{p_i}}{\partial t} = a_p K_G (C_i - \overline{C}_{p_i}) + \psi_i \rho_p r_i \quad (8)$$

where  $\psi_i$  is the stoichiometric coefficient of component  $i$ ,  $\rho_p$  is the particle density and  $r_i$  is the chemical reaction rate.

The global mass transfer resistance is a combination of the resistance in the pores of the catalyst ( $K_p$ ) and the film mass transfer in the external layer of the particles ( $k_f$ ). In this initial assessment, we have assumed that no mass transfer problems exist in the particles and fixed a value of  $K_g = 100$  m/s.

The link between mass and momentum balances is the ideal gas law:

$$p = C_T R_g T \quad (9)$$

$$C_T = \sum_{i=1}^N C_i \quad (10)$$

where  $C_T$  is the total concentration,  $R_g$  is the ideal gas constant and  $T$  is the temperature.

As a first approximation, we have described the reaction rate of oxidation and reduction as first-order to methane and oxygen concentration by:

$$R_{red} = k_{red} C_{CH_4} \quad (11)$$

$$R_{oxid} = k_{ox} C_{O_2} \quad (12)$$

### 3.2 Results from the reactor modeling

The simulation results obtained with the mathematical model for different inlet flow rates and rotation frequency are also shown in Figure 2 (solid lines). The results obtained from the modeling are in close agreement with the experimental results. The reaction kinetics are quite fast thus cyclic steady state is obtained within less than 5 minutes for all conditions tested. The meshing grid used for the simulation coupled with the important number of gases makes each simulation last 15-25 minutes (and consuming ~10GB of RAM memory).

<Figure 4>

It has been observed that the bed dispersion in the bed is a very important factor in controlling the CO<sub>2</sub> purity. In fact, when all operating conditions are ideal (even velocity in all sectors and the same pressure in both boundaries), the gas dispersion in the bed together with methane conversion in the catalyst are the most important factors to define the overall CO<sub>2</sub> purity obtained in the rotating bed reactor.

Keeping all operating conditions constant and reducing the overall flow rate while keeping the methane flow constant results in a net increase of methane concentration within the bed, which is the reason why the CO<sub>2</sub> purity increases. In the previous communication [15] it was also observed that increasing the amount of methane (by increasing its concentration) in the feed step resulted in an increased CO<sub>2</sub> purity.

When the rotational frequency increases, more N<sub>2</sub> from the air section is able to pass through the inert section and get mixed with the CO<sub>2</sub> stream. For higher rotation velocities, the gas experiences an increased angular velocity that makes CO<sub>2</sub> be depleted into the air section: The flow rate in the inert section will not be enough to remove CO<sub>2</sub> in the proper section. However, at low rotation frequencies this effect should be small. For the prototype

reactor the two separation walls in the exit chamber are displaced around 20° to compensate for the rotation. The effect of this is clearly seen in both the experimental and simulation results given in Figure 2 by an optimal rotation frequency of around 2 rotations/min.

An important variable in the CO<sub>2</sub> purity is the amount of gas used in the two inert sectors. At the rotation frequencies used in the experiments, the gas dispersion in the bed, particularly its angular component (dominated by molecular diffusivity), is determinant in mixing the N<sub>2</sub> (and some O<sub>2</sub>) into the CO<sub>2</sub> stream, controlling the final CO<sub>2</sub> purity..

By using an asymmetric velocity in the inert section, the entire velocity and pressure profiles are modified and then the effect of bed dispersion will be completely changed. The results obtained with different inert flow rates are shown in Figure 4. In this case, the efficiency of the inert gas is quite clear since the CO<sub>2</sub> purity doubles when more inert gas is used to "break" the bed angular dispersion tendency to mix the air into the CO<sub>2</sub> exit.

#### 4 Discussion

The developed mathematical model is able to describe the major features of the rotating reactor in terms of mass and momentum transfer. The initial input of the mathematical model is regarding the fluid dynamics of the reactor. It has been observed that bed dispersion (particularly its angular component) is more important than molecular diffusion in the interfaces. For this reason, an efficient way to control CO<sub>2</sub> purity will be to reduce angular dispersion. Solutions to this problem can be to increase the angle of the inert gas sections and/or to introduce physical barriers that structure the catalyst in several compartments reducing angular gas mixing.

It should be pointed out also that the dispersion problems can also be reduced by increasing the overall pressure of the system. The mixing in the system is controlled by dispersion. Typical dispersion equations have the form  $D = D_m + f(v_{gas})$ . If the pressure is higher and similar flow rates are used, the velocity decreases resulting in smaller  $D$ . In addition, increasing the pressure also will lower the dispersion coefficient since  $D_m \propto p^{-1}$  (Chapman-Enskog theory). Furthermore, as mentioned before, operating at higher pressures may also significantly reduce the overall volume of the reactor making it an interesting alternative for chemical looping combustion.

An important "practical" issue of operating the reactor is the consequence of controlling the even flow rates exiting through the air and CO<sub>2</sub> sectors. In all previous simulations in this study, the pressure at the exit of the reactor was assumed to be atmospheric. However, we have performed some initial tests increasing the pressure of the CO<sub>2</sub> side (just 10 Pa). The velocity profile is shown in Figure 5 and compared to the velocity profile using symmetric pressure at the exit. The gas flow pattern changes considerably even with very small

pressure changes. With an "induced" pressure gradient, the CH<sub>4</sub> slightly increases (more CH<sub>4</sub> gets into the air sector producing more CO<sub>2</sub>). Furthermore, a CO<sub>2</sub> purity decrease of 5% is observed.

<Figure 5>

## **5 Conclusions**

A mathematical model of the rotating bed reactor designed for chemical looping combustion has been developed. Since the main challenge with this reactor type is internal gas mixing reducing the purity of CO<sub>2</sub> in the fuel effluent gas stream, the main aim has been to simulate the gas composition at various points in the reactor taking gas diffusion within the oxygen carrier and the voids into consideration. The model has been validated against the experimental results obtained with the prototype reactor: The observed trends when changing process parameters such as total gas flow, rotation frequency, inert gas flow as well as pressure differences between the two reactor exits are nicely reflected by the model. A next step will be to use the model to find ways to change the reactor design and oxygen carrier particle characteristics in order to improve the reactor performance.

## **Acknowledgements**

This publication is produced with support from the BIGCCS Centre, performed under the Norwegian research program Centers for Environment-friendly Energy Research (FME). The authors acknowledge the following partners for their contributions: Aker Solutions, ConocoPhillips, Det Norske Veritas AS, Gassco AS, GDF SUEZ, Hydro Aluminium AS, Shell Technology AS, Statoil Petroleum AS, TOTAL E&P Norge AS, and the Research Council of Norway (193816/S60).



## Glossary

|                  |  |
|------------------|--|
| CLC              | Chemical looping combustion            |
| CFB              | Circulating fluidized bed              |
| FCC              | Fluidized catalytic cracking           |
| $\Delta H^\circ$ | Standard enthalpy of reaction          |
| $\varepsilon_c$  | <i>Bed porosity</i>                    |
| $\kappa_r$       | permeability                           |
| $\rho$           | gas density                            |
| $\rho_p$         | particle density                       |
| $p$              | pressure                               |
| $\eta$           | gas viscosity                          |
| $C_i$            | gas concentration of component i       |
| $u$              | linear gas velocity                    |
| $v_{\text{gas}}$ | gas velocity                           |
| $D$              | dispersion coefficient                 |
| $D_m$            | Molecular diffusion coefficient        |
| $D_r$            | radial dispersion coefficient          |
| $t$              | time                                   |
| $\delta_{TS}$    | time coefficient                       |
| $R$              | transfer rate to catalyst              |
| $r_i$            | reaction rate of component i           |
| $a_p$            | area to volume ratio                   |
| $R_p$            | catalyst radius                        |
| $\psi_i$         | Stoichiometry coefficient of comp. i   |
| $K_g$            | total diffusion resistance             |
| $K_p$            | diffusion resistance in the pores      |
| $k_f$            | diffusion resistance in the surf. film |
| $C_T$            | total concentration                    |
| $R_g$            | ideal gas constant                     |
| $T$              | Absolute temperature                   |
| $k_{\text{red}}$ | rate constant of reduction reaction    |
| $k_{\text{ox}}$  | rate constant of oxidation reaction    |

$\overline{C}_{p_i}$  Average concentration of component i inside the pores

$\omega$  Angular velocity

## Figure captions:

**Figure 1:** The rotating bed prototype reactor: a) Vertical cross-section of the reactor showing the upper and lower water cooling sections and the central reactor unit including the gas feeding (colored) and the two exit sections. b) The central section showing the gas feeding sectors as part of the fixed central axis: Red= fuel feeding sector, blue= the two inert feeding sectors and green= air feeding sector. The two walls dividing the two exit chambers are also shown, while the rotating oxygen carrier bed has been omitted for clarity. c) The un-capped rotating oxygen carrier bed with the 1.5 mm CuO/Al<sub>2</sub>O<sub>3</sub> spheres used.

**Figure 2:** Potential CO<sub>2</sub> purity as a function of: a) Total inlet flow, and b) Rotation frequency. The data is based on reactor tests at 800°C, rotation frequency of 2 rotations/min, total inlet gas flow of 2 L/min, 40 ml/min CH<sub>4</sub> (diluted with argon), and inert gas (argon) flow proportional to the angular size of the inert sector if not otherwise stated.

**Figure 3.** The geometry of the rotating reactor and mesh for solving the PDEs equations. The CuO/Al<sub>2</sub>O<sub>3</sub> spheres are placed in sections 1a-1d. The major components of the two exit gases are shown with "slipped" components in brackets.

**Figure 4:** Potential CO<sub>2</sub> purity as a function of different inlet ratio of inert gas (right). The data is based on reactor tests at 800°C, rotation frequency of 2 rotations/min, total inlet gas flow of 2 L/min, 40 ml/min CH<sub>4</sub>. To the left the CO<sub>2</sub> concentration profile in cyclic steady state is shown for the higher purity case.

**Figure 5:** Velocity field of rotating bed reactor using (a) same exit pressure in both ends, and (b) with increased pressure in the CO<sub>2</sub> end.

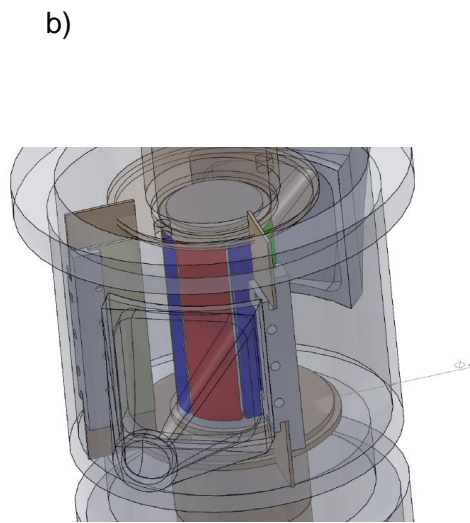
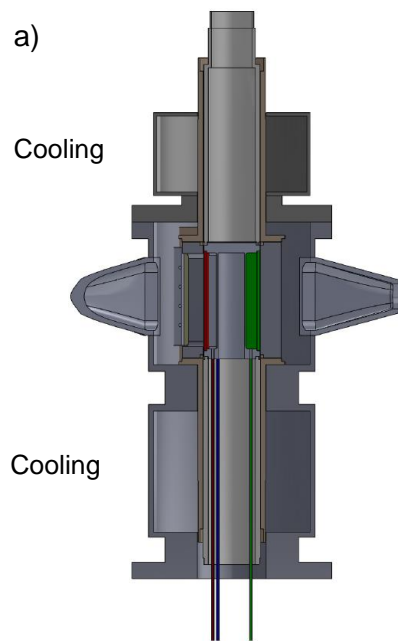


**Figure 1**

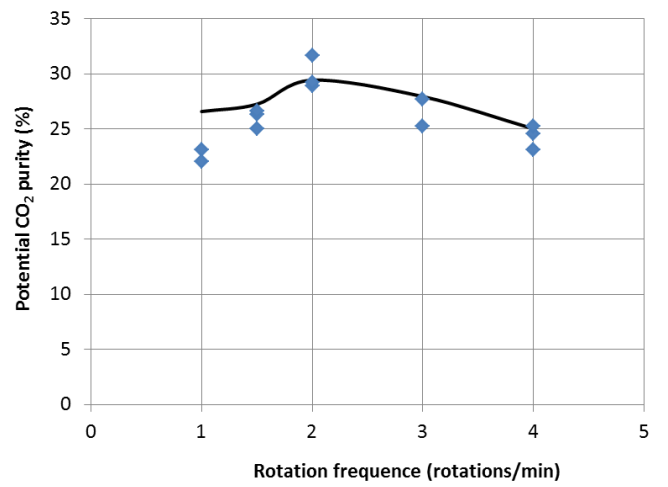
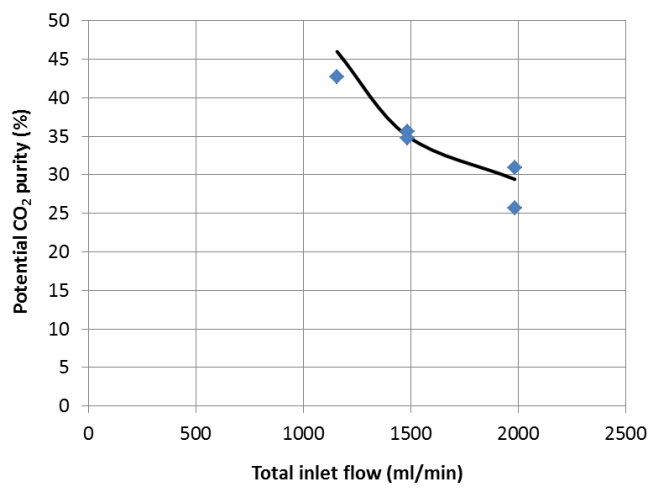


**Figure 2**

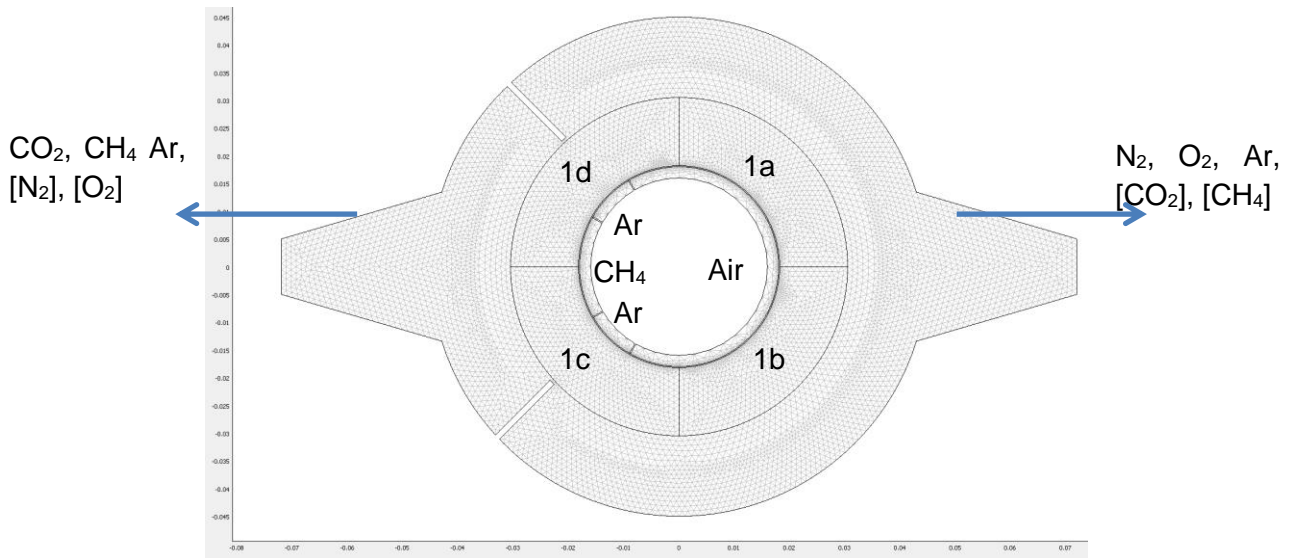


**Figure 3**

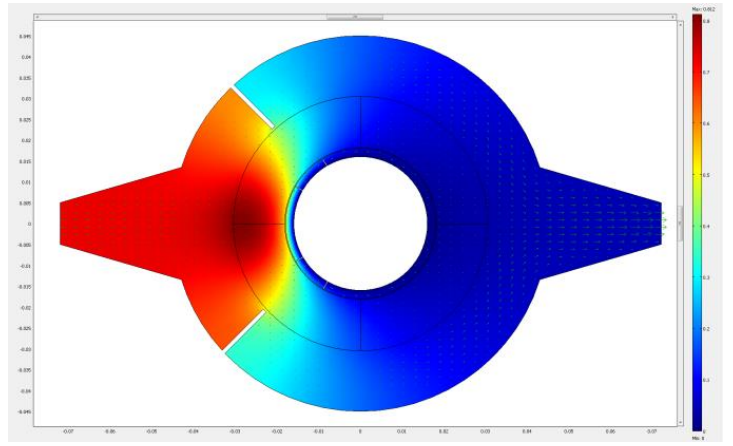
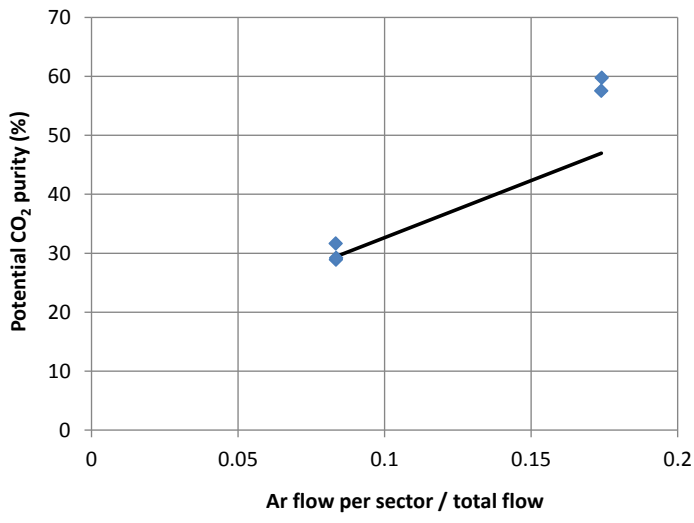


**Figure 4**

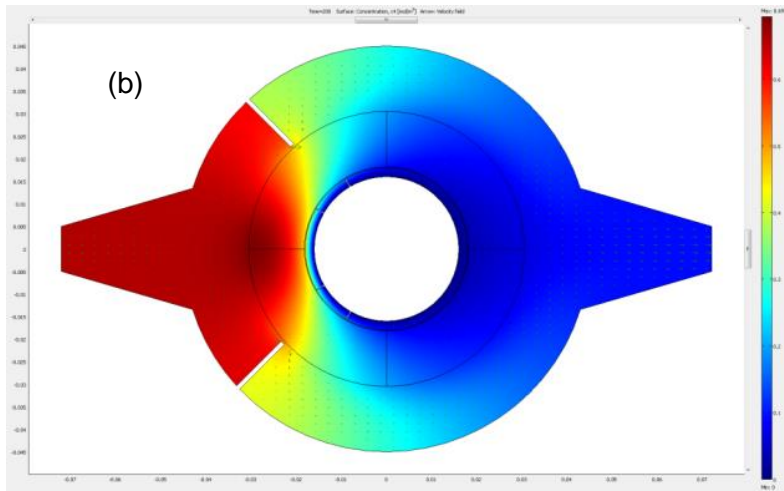
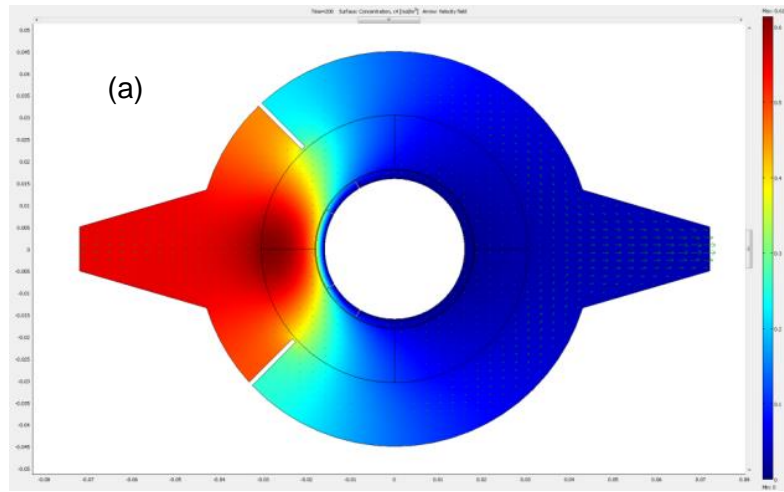


Figure 5

## References

---

- [1] Lewis WK, Gilliland ER. Production of pure carbon dioxide. S.O.D. Company, US Patent: 2,665,971, 1954.
- [2] Richter H, Knoche K. Reversibility of combustion process. *ACS Symposium Series* 1983;235:71-85.
- [3] Ishida M, Jin H. A novel combustor based on chemical-looping combustion reactions and its reactions kinetics. *J. Chem. Eng. Jpn.* 1994;27: 296- 301.
- [4] Kvamsdal HM, Jordal K, Bolland O. A quantitative comparison of gas turbine cycles with CO<sub>2</sub> capture. *Energy* 2007;32:10-24.
- [5] Erlach B, Schmidt M, Tsatsaronis G. Comparison of carbon capture IGCC with pre-combustion decarbonisation and with chemical-looping combustion, *Energy* 2011;36:3804-3815.
- [6] Ekstrom C, Schwendig F, Biede O, Franco F, Haupt G, de Koeijer G, Papapavlou C, Røkke PE. Techno-Economic Evaluations and Benchmarking of Pre-combustion CO<sub>2</sub> Capture and Oxy-fuel Processes Developed in the European ENCAP Project. *Energy Proc.* 2009;1: 4233-4240.
- [7] Hossain MM, de Lasa HI. Chemical-looping-combustion (CLC) for inherent CO<sub>2</sub> separations-a review. *Chem. Eng. Sci.* 2008;63(18):4433-4451.
- [8] Fan LS, Wang WL, Luo SW., (2012), Chemical looping processes for CO<sub>2</sub> capture and carbonaceous fuel conversion - prospect and opportunity. *Eng. Environ. Sci.* 2012;5(6);7254-7280.
- [9] Adanez J, Abad A, Garcia-Labiano F, Gayan P, de Diego LF. Progress in Chemical-Looping-Combustion and Reforming technologies. *Prog. in Energ. Comb. Sci.* 2012;38(2);215-282.
- [10] Zeng L, Luo SW, Sridhar D, Fan LS. Chemical looping processes - particle characterization, ionic diffusion-reaction mechanism and reactor engineering. *Rev. Chem. Eng.* 2012;28(1):1-42
- [11] Berguerand N, Lyngfelt A. Batch testing of solid fuels with ilmenite in a 10 kWth chemical-looping combustor. *Fuel* 2010;89:1749-1762 – and references therein.
- [12] Pröll T, Kolbitsch P, Bolhàr-Nordenkampf J, Hofbauer H. A novel dual circulating fluidized bed system for chemical looping combustion. *AIChJ.* 2009;55:3255-3266.
- [13] Jin H, Ishida M. Reactivity study on natural-gas-fueled chemical-looping combustion by a fixed-bed reactor. *Ind. Eng. Chem. Res.* 2002;41:4004-4007.
- [14] Dahl IM, Bakken E, Larring Y, Spjelkavik AI, Håkonsen SF, Blom R. On the development of novel reactor concepts for chemical looping combustion. *Energy Proc.* 2009;1:1513-1519.



- 
- [15] Hakonsen SF; Blom R. Chemical Looping Combustion in a Rotating Bed Reactor - Finding Optimal Process Conditions for Prototype Reactor. *Environ. Sci. Technol.* 2011;45:9619-9626.
- [16] Pavone D. CO<sub>2</sub> capture by means of chemical looping combustion. In Proceedings of the COMSOL Multiphysics User's Conference. Paris, France, 2005
- [17] Zhao Z, Chen T, Ghoniem AF. Rotary Bed Reactor for Chemical-Looping Combustion with Carbon Capture: Reactor Design and Model Development. *Energy & Fuels* 2013;27:327-343..